

Surface diffusion and surface growth in nanofilms of mixed rocksalt oxides†

D. J. Harris,^{*a} T. S. Farrow,^a J. H. Harding,^b M. Yu. Lavrentiev,^c N. L. Allan,^d W. Smith^e and J. A. Purton^f

^a Department of Physics and Astronomy, University College London, London, UK WC1 6BT
E-mail: Duncan.Harris@ucl.ac.uk; Fax: 020 7679 1360; Tel: 020 7679 3400

^b Department of Engineering Materials, University of Sheffield, Sheffield, UK S1 3JD.
E-mail: j.harding@sheffield.ac.uk; Fax: 0114 222 5843; Tel: 0114 222 5957

^c Department of Chemistry, University of Bristol, Bristol, UK BS8 1TS.
E-mail: m.lavrentiev@bris.ac.uk; Fax: 0117 925 1295; Tel: 0117 954 6863

^d Department of Chemistry, University of Bristol, Bristol, UK BS8 1TS.
E-mail: n.l.allan@bris.ac.uk; Fax: 0117 925 1295; Tel: 0117 928 8308

^e Computational Science & Engineering, CCLRC Daresbury Laboratory, Cheshire, UK WA4 4AD E-mail: w.smith@dl.ac.uk; Fax: 01925 603634; Tel: 01925 603257

^f Synchrotron Radiation, CCLRC Daresbury Laboratory, Cheshire, UK WA4 4AD.
E-mail: j.a.purton@dl.ac.uk; Fax: 01925 603100; Tel: 01925 603785

Received 30th November 2004, Accepted 15th February 2005
First published as an Advance Article on the web 7th March 2005

We have modelled the surface diffusion and growth of BaO and SrO both in the homoepitaxial and heteroepitaxial (BaO on SrO and SrO on BaO) cases. The diffusion proceeds most favourably by an exchange mechanism involving the surface layer. When impurities are adsorbed on the surface this can lead to intermixing between the layers. This strongly suggests that ionic materials may not be grown on a substrate with a similar structure without significant intermixing. Island growth begins with the formation of individual clusters which grow and merge together.

Introduction

A recent review on surface diffusion in metals¹ emphasises the importance of exchange mechanisms.^{2,3} Recently, we⁴ have shown that similar mechanisms are also important in surface diffusion in some oxides of the rocksalt structure. Such mechanisms should cause mixing when one oxide is grown on top of another. This is an important issue in the growth of oxide layers by molecular beam epitaxy where the commonest smoothing mechanism is surface diffusion. In many applications, atomically sharp layers are desirable and often essential.

The usual method of simulating surface diffusion is molecular dynamics. This is suitable for fast-ion conductors but for simple basic oxides, where the migration barriers are high, the timescales required for direct simulation at temperatures of interest are too long to achieve suitable statistics in a reasonable time frame. An alternative is to use Kinetic Monte Carlo (KMC) methods, but this requires that the diffusion mechanisms and activation energies are fully known in advance, something that is not usually possible in even the simplest systems.

Voter and coworkers⁵ have recently developed a variety of methods to deal with the long timescale problem under the general label of 'hyperdynamics'. The most robust of these, Temperature Accelerated Dynamics (TAD),^{6,7} first calculates the individual rates for all of the exit routes from a single energy basin at high temperature. It then extrapolates this information to the low temperature of interest, thus correctly

accounting for the different behaviour of the various contributing mechanisms with temperature. The method needs no previous knowledge of the diffusion mechanism and thus provides an *unbiased* calculation of the diffusion rate. The method gives greatly enhanced simulation times at the cost of assuming the validity of transition state theory. Detailed information on the trajectory at short times is lost while the correct behaviour of the trajectory at the longer times of interest is retained. A brief description of the method will be given later; for full details see the references (*e.g.*, ref. 6). To obtain even longer simulation times, we have extended the method by using TAD to generate a complete set of diffusion mechanisms and rates for use as the input to a KMC calculation.

BaO and SrO are of particular interest since both of these materials have a dielectric constant high enough to be of use as a gate dielectric. In this paper we consider the effect of mixing during the growth of one oxide on another.

Methods; temperature accelerated dynamics

Temperature Accelerated Dynamics (TAD) uses simulations performed at high temperature to give the evolution of a system at a lower temperature of interest. We present here only a brief summary. The method assumes that ionic motion occurs by a hopping mechanism and that transition state theory is valid, but does not assume anything about the particular mechanisms involved. It uses a molecular dynamics simulation performed at high temperature to identify transitions from one energy basin to the next. When a transition is detected, the molecular dynamics simulation is halted. The saddle point, the highest point on the minimum energy path

† Presented at the 84th International Bunsen Discussion Meeting on the Structure and Dynamics of Disordered Ionic Materials, Münster, Germany, October 6–8, 2004.

between the basins, is located using a Nudged Elastic Band calculation^{8,9} and the migration energy determined from the difference in the energy of the saddle point and that of the minimum of the initial basin. The trajectory is then reflected back into the starting basin and the simulation continued from the point where the trajectory crosses the dividing surface between the two basins but with the velocities of all particles reversed. A Langevin thermostat injects some noise into the trajectory so that the previous path is not retraced.

From the basin-constrained dynamics, we can extract a series of waiting times (times before a particular transition). For systems where events are infrequent, as here, we can assume first-order kinetics and therefore the waiting times for a particular transition are exponentially distributed with a probability distribution

$$f(t)dt = \Gamma \exp(-\Gamma t) dt \quad (1)$$

where Γ is the transition rate, here described by

$$\Gamma = \Gamma_0 \exp(-u_m/k_B T) \quad (2)$$

where u_m is the migration energy, k_B is Boltzmann's constant and T is the temperature. An essential step in the TAD argument is⁶ that a molecular dynamics simulation is equivalent to drawing random wait times for each possible transition from the probability distribution (1) and only using the shortest. From (1) and (2) it is possible to show^{6,7} that low-temperature waiting times can be extrapolated from high-temperature waiting times obtained from the simulation using

$$t_{\text{low}} = t_{\text{high}} \exp(u_m [T_{\text{low}}^{-1} - T_{\text{high}}^{-1}] / k_B) \quad (3)$$

The distribution of the waiting times at the low temperature is the same as the distribution at the high temperature. Thus a low-temperature sequence of events equivalent to an MD simulation can be constructed from the high-temperature sequence by using (3) to extrapolate the waiting times and picking the shortest. This is shown in Fig. 1. From the diagram, we can also see that the waiting times for processes (1) and (2) can change their order between high and low temperatures if $u_{m2} < u_{m1}$.

For practical simulations, we require a criterion that will enable us to decide when to stop the high-temperature simulation for a given basin. We assume that there is a lowest possible prefactor (in eqn. (2)) for the system, $\Gamma_{0,\text{min}}$. It can then be shown⁶ that $v_{\text{min}} = \Gamma_{0,\text{min}} / \ln(1/\delta)$ gives an effective (reciprocal) waiting time at infinite temperature (to within a confidence δ) for a process with the assumed minimum prefactor. Let us call this the minimum process. We can use this minimum process value, and the value of the shortest current waiting time at low temperature (*i.e.* process 2 in the Fig. 1) to obtain an activation

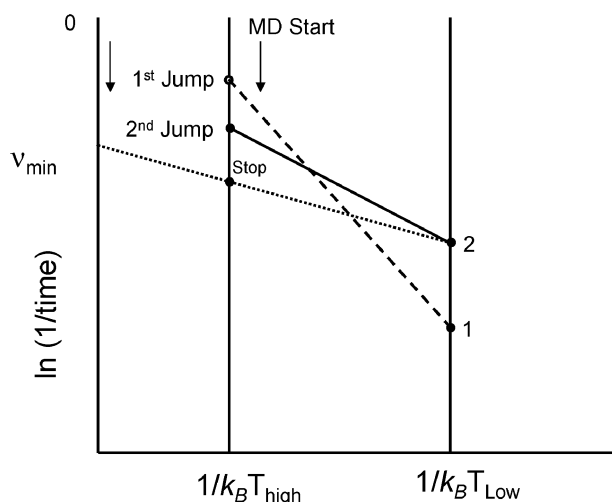


Fig. 1 Schematic showing the progress of a TAD calculation.

Table 1 Short-range Buckingham potentials for the TAD simulations

Interaction	A/eV	$\rho/\text{\AA}$	$C/\text{eV \AA}^6$
$\text{Ba}^{2+}-\text{O}^{2-}$	905.7	0.3976	0.0
$\text{Sr}^{2+}-\text{O}^{2-}$	959.1	0.3721	0.0
$\text{O}^{2-}-\text{O}^{2-}$	22764.0	0.149	27.88

energy. This is the minimum activation energy for a process that has a longer waiting time than process 2 at high temperature while still having a waiting time the same as process 2 at low temperature. We can obtain a waiting time for the minimum process at the high temperature of the simulation by interpolation (labelled stop in Fig. 1). The point is, provided we run the high-temperature simulation until the stop time, we have a procedure which guarantees that we will find the mechanism with the shortest wait time at low temperature to within a given confidence δ . The choice of $\Gamma_{0,\text{min}}$ is clearly important: too high a value and we may miss a process at low temperature; too low a value and we waste computer time.

The TAD calculation can then be used as a direct simulation of diffusion. When we have run the high temperature simulation as long as the stop time, we change the system according to the first mechanism that occurs at the lower temperature (process 2), advance the simulation clock by the extrapolated time before this mechanism happened and restart the high-temperature simulation using the new configuration. This can provide large enhancements of the effective simulation time, in favourable cases of the order of 10^5 . Alternatively, as here, we can use the method to collect an unbiased list of mechanisms together with the appropriate rates to be used as the input for a kinetic Monte Carlo simulation. This allows us to simulate even longer periods of time at low temperature.

Our TAD calculations used a rigid ion model with full ionic charge and short-range Buckingham potentials:

$$V(r) = A \exp(-r/\rho) - Cr^{-6} \quad (4)$$

where r is the interionic separation and A , ρ and C are the potential parameters. Values were taken from ref. 10 and are given in Table 1. A 10 \AA cutoff was used. The long range forces were calculated using the Ewald summation.

The surface was represented by a slab of ions, periodically repeated in three dimensions, with a 12 \AA gap between slabs in the stacking direction to prevent inter-slab interactions. The slabs typically contained approximately 400 ions, giving five layers of ions in the slab. The high and low temperatures were set to 1400 and 300 K, respectively. Since we were interested in obtaining a full set of escape routes for use in the KMC calculation rather than simulating the diffusion directly, we set a low minimum prefactor of 5×10^{11} Hz since we wish to capture all the processes and not simply identify the one with the shortest waiting time. For a pure TAD calculation a prefactor ten times larger might be more suitable since this is typical of the values of prefactors in diffusion. While we could use the lower prefactor, it would be at the cost of greatly increased simulation time.

Results from TAD simulations

The (100) surface

In our previous work⁴ we showed that the lowest energy hopping mechanism on a (100) surface of BaO involved an exchange process, as Fig. 2 shows. During the first stage of the mechanism the adsorbed oxide ion (for example) moves towards the surface and to one side of the adsorbed cation whilst the oxide ion in the surface layer directly beneath the adsorbed cation moves out of the surface and to the opposite side of the cation to the first oxide, forming an oxide-cation-oxide trimer on the surface with the oxide ions midway between the surface

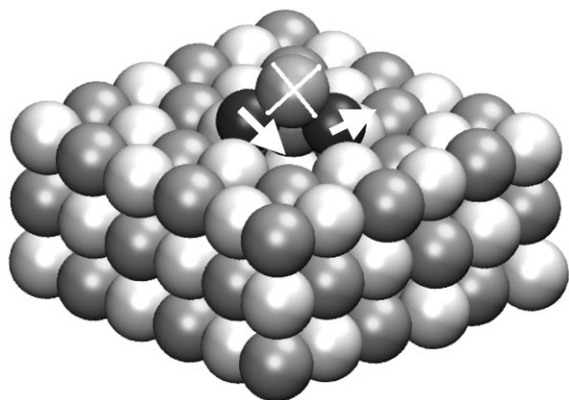


Fig. 2 Exchange mechanism for oxide diffusion in the (100) surface. White spheres are cations, grey are oxide. The top (crossed) is the surface cation. Dark spheres are the oxide ions involved in the exchange.

and adsorbed layer. The second stage of the exchange involves one of the two oxide ions moving back into the surface layer whilst the other moves to an adsorbed position. Symmetry gives four configurations, only two of which are proper exchanges with an oxide ion that was previously in the surface layer. An alternative second stage moves one of the exchanging pair back into the surface layer, whilst the adsorbed counter ion moves out to a midway position, resulting in the situation found at the end of the first stage of the simple pair hopping mechanism. The second mechanism involves a concerted hop of both ions to a pyramidal sublattice site midway between surface lattice sites above the surface. A second concerted hop then moves them onto another pair of surface lattice sites. Symmetry allows for four possible end configurations to this jump.

Table 2 gives the calculated activation energies for these processes for ion pairs on the pure (100) surfaces of SrO and BaO. There is little variation in the activation energy with cation size for the initial stage of the cation exchange process. The oxide exchange is the favoured process in both cases. The diffusion process in BaO and SrO thus consists of the ions in the adsorbed pair taking individual steps across the surface, but with frequent exchanges of ions to and from the surface layer. Some preliminary calculations with shell models for the

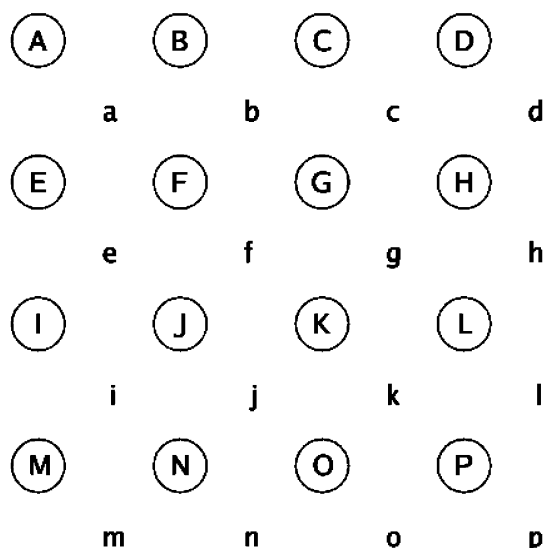


Fig. 3 Labelling scheme used in Tables 2 and 3. Upper case letters refer to the ion sites, lower case letters to the interstitial sites. *ads* refers to an ion adsorbed above the surface; *sfc* refers to an ion in the surface layer; *stp* refers to an ion in the step edge. Hence $O(G_{\text{ads}}) \rightarrow b$ means that an oxygen ion adsorbed on a lattice site at G moves to an interstitial site at b.

activation energies of jumps ζ and η for the BaO case show only small differences. The activation energy of ζ is raised by 0.08 eV and that of η lowered by 0.04 eV.

One important consequence of this is possibility of mixing in the case of impurities on a crystal surface. To investigate impurity embedding we set up two simulation cells; one consisted of a SrO pair on a BaO surface, whilst the other contained a BaO pair on a SrO surface. For BaO on SrO no embedding was found due to the limited space available in the surface layer for the barium ion. However, the cation exchange in this case was more favourable than the oxide exchange (0.41 eV for Ba compared to 0.48 eV for O) and lower than in the homogeneous case. For SrO on BaO, the first stage of cation exchange was unfavourable compared to oxygen exchange (0.60 eV for Sr compared to 0.39 eV for oxygen). This suggests that the strontium ion will pin the system to some extent. The oxygen ion will simply rotate around the Sr ion until the Sr ion

Table 2 Activation energies (in eV) for stage 1 and 2 exchange and pair hopping on (100) surfaces for homogeneous and heterogeneous systems. For site nomenclature see Fig. 3

Jump label	Jump description	SrO	BaO	SrO on BaO	BaO on SrO
Stage 1: $M(F_{\text{ads}}), O(G_{\text{ads}})$					
α	$O(G_{\text{ads}}) \rightarrow b O(F_{\text{sfc}}) \rightarrow e$	0.378	0.340	0.39	0.48
β	$M(F_{\text{ads}}) \rightarrow f M(G_{\text{sfc}}) \rightarrow c$	0.407	0.362	0.60	0.41
γ	$M(F_{\text{ads}}) \rightarrow a O(G_{\text{ads}}) \rightarrow b$	0.430	0.399	0.68	0.49
Stage 2: $M(F_{\text{ads}}), O(b,e)$					
δ	$O(b) \rightarrow F_{\text{sfc}} O(e) \rightarrow J_{\text{ads}}$	0.362	0.365	0.41	0.35
ϵ	$O(e) \rightarrow F_{\text{sfc}} M(F_{\text{ads}}) \rightarrow a$	0.32	0.38	0.53	0.27
Stage 2: $O(G_{\text{ads}}), M(c,f)$					
ζ	$M(c) \rightarrow G_{\text{sfc}} M(f) \rightarrow K_{\text{ads}}$	0.345	0.35	0.41 (Ba ads) 0.71 (Sr ads)	0.11 (Ba ads)
η	$M(f) \rightarrow G_{\text{sfc}} O(G_{\text{ads}}) \rightarrow b$	0.35	0.36	0.39 (Ba ads) 0.49 (Sr ads)	0.23 (Ba ads)
Stage 2: $M(a), O(b)$					
θ	$M(a) \rightarrow F_{\text{ads}} O(b) \rightarrow G_{\text{ads}}$	0.345	0.359	0.65	0.34

Table 3 Activation energies (in eV) for migration near a step on a (710) surface for homogeneous and heterogeneous systems. For site nomenclature see Fig. 3 (the step is along A–B–C–D). In the mixed cases M' is the impurity ion; otherwise M' = M

Jump label	Start position	Jump description	SrO	BaO	SrO on BaO	BaO on SrO
Step edge positions: positions E to P in Fig. 3 on lower terrace						
ι	M'(F _{ads}), O(G _{ads})	M(C _{stp}) → H _{ads}	0.736	0.683	0.81	0.69
		O(B _{stp}) → E _{ads}	0.735	0.683	0.64	0.78
κ	M'(F _{ads}), M(H _{ads}), O(G _{ads})	M(H _{ads}) → C _{stp}	0.152	0.143	0.14	0.23
		M(F _{ads}) → C _{stp}			0.34	
λ	M'(F _{ads}), O(E _{ads} , G _{ads})	O(E _{ads}) → B _{stp}	0.153	0.143	0.14	0.20
μ	M(J _{ads}), O(f,i)	O(f) → F _{ads} O(i) → J _{sfc}	0.242	0.253		
		O(f) → K _{ads} O(i) → J _{sfc}	0.207	0.199		
		O(f) → J _{sfc} O(i) → N _{ads}	0.273	0.235		
Terrace jumps: positions E to P in Fig. 3 on higher terrace						
ν	M(J _{ads}), O(f,i)	O(f) → F _{ads} O(i) → J _{sfc}	0.36	0.37		
		O(f) → K _{ads} O(i) → J _{sfc}	0.16	0.30		
		O(f) → J _{sfc} O(i) → N _{ads}	0.26	0.31		

becomes embedded into the surface. The resulting BaO pair will then be able to move away. The Sr embedding process is greatly favoured as the second stage of the exchange (0.44 eV for Sr implantation compared to 0.71 eV for Ba implantation). Although previous simulations have noted this intermixing, they were unable to determine the mechanism.¹¹

The (710) stepped surface

The (100) hopping mechanisms have several symmetry related end structures. The presence of a step edge removes much of this symmetry and thus complicates the process. The second stage of the exchange mechanism can move the ion pair towards, away from or parallel to the step edge. Our calculations showed that in the homogeneous systems the stage two activation energy to move parallel to the step is smaller than that for moving towards or away from the step (see Table 3). The simple pair hopping mechanism shows a similar splitting of energies. Analogous behaviour is found for ions moving on the terrace above the step edge. However, when the first stage of the exchange occurs within two atomic spacings from the step there is a general rearrangement as the ions in the step edge are pushed out and the moving ions fall down into the resulting space (Fig. 4). The activation process is very low –0.03 eV.

Ion pairs that reach the step edge remain bound to the step. Motion along the step edge is possible by an exchange mechanism where an ion in the step edge leaves to form a vacancy. This

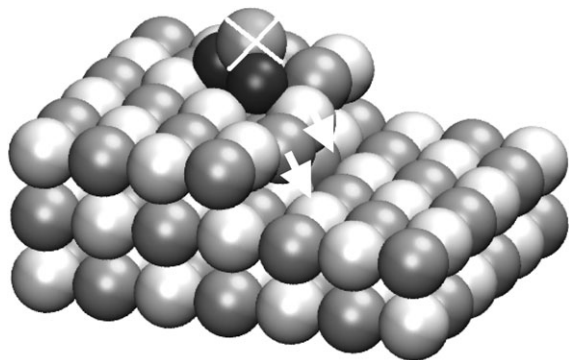


Fig. 4 The collapse of a BaO step due to an exchange in the terrace above it. The top (crossed) sphere is the surface cation whilst the two dark spheres are the oxide ions involved in the exchange.

is then filled by either the original ion or the equivalent ion from the adsorbed pair. The energy for the first stage of this process is relatively high (≈ 0.7 eV), whilst the return energy is much lower (≈ 0.2 eV) as shown in Table 3. The (100) exchange mechanism is not seen when the ion pair is attached to the step.

Impurities complicate the situation further. As in the (100) case a strontium ion on a BaO surface can become embedded within the surface layer. For motion next to the step edge a slight imbalance in the energies for impurity and lattice ion motion is found (Table 3). For BaO on SrO the barium ion is unable to penetrate the step edge, resulting in the ion pair being pinned.

Kinetic Monte Carlo simulations

The activation energies calculated using TAD were used as input for the KMC simulations. The KMC simulations used a single layer surface with 20×20 ions. Two dimensional (2D) periodic boundary conditions were applied. Typical simulations lasted for 4×10^6 events. We use a simple Arrhenius expression (eqn. (1)) for the rate. At each step, an event is chosen with a probability proportional to its rate. The system is changed accordingly, and the time counter advanced by

$$\Delta t = -\ln \mu / \sum_i \Gamma_i \quad (5)$$

where μ is a uniform random number in the interval [0,1] and $\sum_i \Gamma_i$ is the sum over all possible events.

However, to calculate the rates, we require the prefactors. (They are not required in the TAD calculation except to define the length of the simulation through the stop time. They are required in KMC because the dynamics is expressed only through the rates). Within transition state theory, the prefactors can be obtained from Vineyard's¹² theory, given the lattice frequencies for the ground state and saddle-point configurations of the jump. The prefactor is given by eqn. (6).

$$\Gamma_0 = \frac{\prod_{i=1}^N \nu_i}{\prod_{j=1}^{N-1} \nu'_j} \quad (6)$$

where ν_i are the frequencies for the ground state and ν'_j are the frequencies at the saddle point. The product is performed over the total number of modes N for the ground state and $N-1$ for the saddle point (the mode corresponding to the reaction coordinate has imaginary frequency). We know both ground state and saddle point configurations from the previous calculations, and calculate the frequencies required by diagonalising

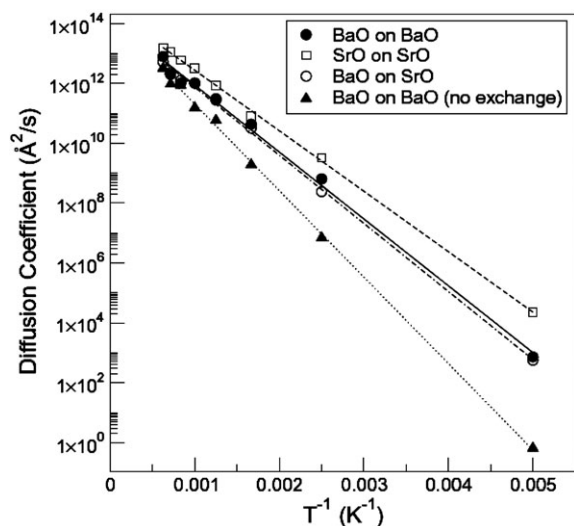


Fig. 5 Diffusion coefficients for oxide ion pairs as a function of temperature.

the Hessian in both cases using quasiharmonic lattice dynamics and the code SHELL.¹³ This is a practicable task for the simple exchange configurations; however for the step configurations the size of the matrices to diagonalise presents serious numerical problems. We have therefore calculated the prefactors only for the simple surface processes and assumed that the prefactors for processes near steps are equal to those of the corresponding surface process. Since *all* the prefactor values calculated are equal to within about a factor of two, we do not consider this approximation likely to give a serious error.

First, we investigated diffusion-like motion of a single ion pair on the (100) surface of the same or another rocksalt oxide. The isotropic diffusion coefficient, D , for the 2D movement can be obtained from $4Dt = \langle r^2 \rangle$, using the data from Tables 2 and 4 to calculate the rates. These coefficients are plotted in Fig. 5. As the activation energy data suggests, the diffusion coefficient for SrO on SrO is larger than for BaO on BaO. In order to estimate the effect of including exchange mechanisms, we also evaluated and plotted the diffusion coefficient data for BaO on BaO without taking into account that mechanism. This results in a 1–3 order of magnitude reduction of the diffusion coefficient, depending on the temperature. A similar, although less pronounced, effect was found for SrO on SrO. The diffusion coefficient for the motion of a BaO pair on the surface of SrO, also shown in Fig. 5, is very close to that for the motion of BaO on BaO.

For a SrO ion pair on the surface of BaO, we have already noted that the second stage of exchange process greatly favours embedding of the strontium atom into the BaO layer. In KMC simulations of SrO on BaO, it means that after a few steps the strontium ion moves into the surface and is replaced by a barium ion. After that, the BaO ion pair continues diffusion-like motion on the surface, while the strontium ion remains embedded in the BaO layer. This effect shows that ionic materials may not be grown on a substrate with a similar structure without significant intermixing, which could compli-

Table 4 Calculated prefactors for jumps in BaO and SrO diffusion (THz). Jump labels refer to Table 2

Jump description	Jump label	SrO	BaO
Anion exchange	α	2.18	1.17
	δ	3.43	2.79
Cation exchange	β	1.46	0.92
	ζ	2.17	1.26
Pair hopping	γ, θ	1.40	2.62

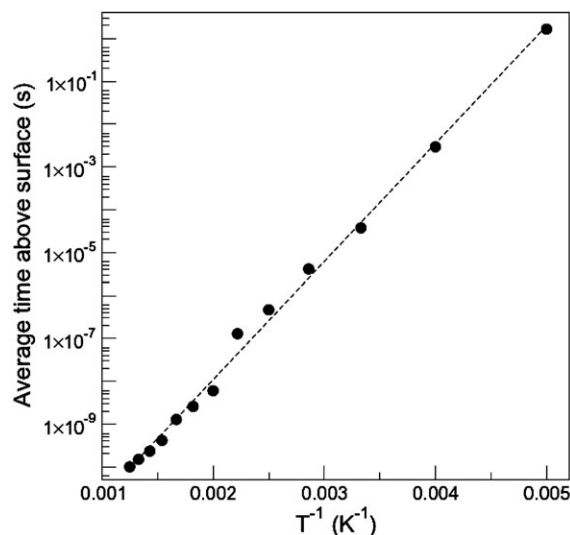


Fig. 6 Average time spent by an Sr ion on a BaO surface before it becomes embedded in the surface.

cate or even make impossible the creation of atomically sharp interfaces between oxides. In Fig. 6 we plot the average time spent by a strontium ion above the surface before it is embedded, as a function of temperature.

The long timescale available with KMC calculations together with the TAD results obtained for the stepped surface allow us to calculate the mean formation time of islands and clusters on the surface, starting from a random distribution of ion pairs. In the first stage of evolution, separate randomly moving ion pairs meet and create initial clusters, which are much less mobile. We define the first stage of cluster formation as the stage after which 50% of the individual freely moving ion pairs have coalesced at least into dimers. Using an initial random coverage of 50% (100 ion pairs on our 20×20 surface) we calculated the average duration of the first stage for temperatures ranging from 100 to 800 K for both BaO and SrO. The logarithm of the time required to create an initial set of clusters increases linearly with inverse temperature. The subsequent evolution of the system proceeds *via* movements of ions attached to clusters, not single ion pairs and occurs therefore on a slower timescale. The clusters gradually capture more ions and absorb other clusters in turn, resulting in the spontaneous creation of islands. A stable final configuration is normally reached within a few thousand individual events. The

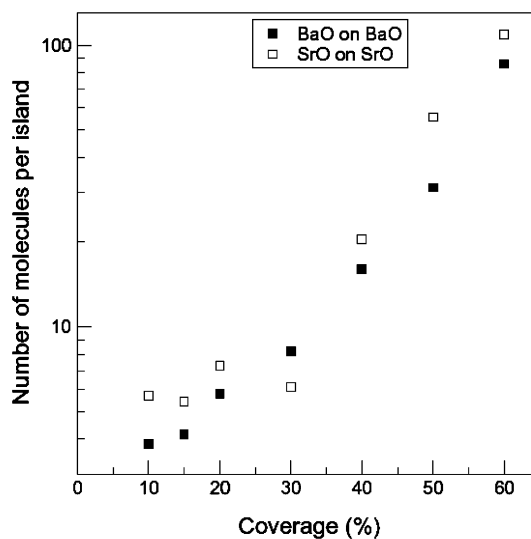


Fig. 7 Average size of surface clusters of BaO and SrO as a function of surface coverage.

average sizes of the surface clusters of BaO on BaO and SrO on SrO are shown in Fig. 7. For low coverages the final configuration contains many small islands; with increasing coverage, the average island size increases. The ability of ion pairs to move on the surface is crucial in reducing the number of defects created when the crystal is grown under deposition. Increasing the average number of movement events taking place between depositions (either by increasing the temperature or by decreasing the deposition rate) dramatically reduces the number of vacancies created in the deposition layer. For example, randomly depositing BaO pairs on BaO surface at a rate of 5×10^6 monolayers s^{-1} created on average one vacancy per eighteen lattice sites at 400 K (with about eleven movement events between two depositions), and only one vacancy per fifty lattice sites at 600 K (with about a hundred movement events between two depositions). We anticipate that exchanges between different deposition layers will help in further reducing the number of vacancies.

Conclusions

Our previous work has shown that exchange mechanisms are a common diffusion mechanism on rocksalt oxide surfaces. This paper has explored one of the consequences of this. For heterosystems where the two ions are of similar size it is highly probable that the adsorbed impurities will mix with the surface layer. This mixing has the added effect of pinning the adsorbed ions at the mixing site. Thus attempts to grow sharp interfaces between different oxides may be complicated if the exchange mechanism is still active in these structures, especially at higher temperatures where the mixing occurs at a faster rate. This is of considerable importance when attempting to grow complex structures using such techniques as MBE (see, for example, the

recent review of Schlom *et al.*¹⁴). Mixing can also give rise to contamination of surfaces, and hence alteration of the surface properties; a significant problem in nanodevices. Ideally, the calculations we have presented should be complemented by *ab initio* investigations of the saddle-point structures that we have obtained here. However, such calculations must involve a large number of ions within the periodic cell to ensure that the effects of strain in the lattice (particularly during the transition) are properly taken into account. Work in this area is currently in progress.

References

- 1 R. Tromp, *Nat. Mater.*, 2003, **2**, 212.
- 2 G. L. Kellogg and P. J. Feibelman, *Phys. Rev. Lett.*, 1990, **64**, 3143.
- 3 C. Chen and T. T. Tsong, *Phys. Rev. Lett.*, 1990, **64**, 3147.
- 4 D. J. Harris, M. Y. Lavrentiev, J. H. Harding, N. L. Allan and J. A. Purton, *J. Phys.: Condens. Matter*, 2004, **16**, L187.
- 5 A. F. Voter, F. Montalenti and T. C. Germann, *Annu. Rev. Mater. Res.*, 2002, **32**, 321.
- 6 M. R. Sorensen and A. F. Voter, *J. Chem. Phys.*, 2000, **112**, 9599.
- 7 F. Montalenti and A. F. Voter, *J. Chem. Phys.*, 2002, **116**, 4819.
- 8 G. Henkelmann, B. P. Uberuaga and H. Jonsson, *J. Chem. Phys.*, 2000, **113**, 9901.
- 9 H. Jonsson and G. Henkelmann, *J. Chem. Phys.*, 2000, **113**, 9978.
- 10 G. V. Lewis and C. R. A. Catlow, *J. Phys. C*, 1985, **18**, 1149.
- 11 D. C. Sayle, C. R. A. Catlow, J. H. Harding, M. J. F. Healy, S. A. Maicaneanu, S. C. Parker, B. Slater and G. W. J. Watson, *J. Mater. Chem.*, 2000, **10**, 1315.
- 12 G. H. Vineyard, *J. Phys. Chem. Solids*, 1957, **3**, 121.
- 13 M. B. Taylor, G. D. Barrera, N. L. Allan, T. H. K. Barron and W. C. Mackrodt, *Comput. Phys. Commun.*, 1998, **109**, 135.
- 14 D. G. Schlom, J. H. Haeni, J. Lettieri, C. D. Theis, W. Tian, J. C. Jiang and X. Q. Pan, *Mater. Sci. Eng. B*, 2001, **87**, 28.